American Mineralogist, Volume 89, pages 1694–1700, 2004

The synthesis of zeolite-P, Linde Type A, and hydroxysodalite zeolites from paper sludge ash at low temperature (80 °C): Optimal ash-leaching condition for zeolite synthesis

TAKAAKI WAJIMA,[1,*] KEIKO KUZAWA,[1] HIROJI ISHIMOTO,[2] OSAMU TAMADA,[1] AND TAKASHI NISHIYAMA[1]

[1]Graduate School of Human and Environmental Studies, Kyoto University, Yoshida-nihonmatsu-cho, Sakyo-ku, Kyoto, Japan
[2]Access Network Service Systems Laboratories, Nippon Telegraph and Telephone Corporation, Hanabatake, Tsukuba, Japan

ABSTRACT

Typically, the ash from incineration of paper sludge contains a high percentage of Ca in the form of anorthite ($CaAl_2Si_2O_8$) and gehlenite ($Ca_2Al_2SiO_7$). The Ca in the sludge originates from calcite that is included in paper as fillers. We applied acid leaching with HCl on the ash to reduce its Ca content. Zeolite was then synthesized from the leached ash through reaction with 2.5 *M* NaOH solution at 80 ºC for 24 hours. The fraction of Ca and Al extracted from the ash correlates with the pH of the leachant. We determined the leachant pH (after 24 hours of leaching) associated with the Ca:Al:Si ratio in the leached ash that provided optimal production of zeolites with high cation-exchange capacity. During acid leaching, gehlenite dissolved out at higher pH than anorthite. In the case of pH > 5, both gehlenite and anorthite remained in the ash, and hydroxysodalite and LTA (Linde Type A) were synthesized in the product. In the case of pH = 1–5 in the leachant, gehlenite dissolved out but anorthite remained in the ash, and LTA and Na-P1 (zeolite-P) were produced. In the case of pH < 1, both gehlenite and anorthite dissolved out, and only Na-P1 was produced. The cation-exchange capacities of the products that contained hydroxysodalite, LTA, and Na-P1 were approximately 130, 200, and 120 cmol/kg, respectively. We conclude that acid leaching of paper sludge ash controls which of the three zeolite phases form, and that LTA and Na-P1 exhibit a higher cation-exchange capacity than hydroxysodalite. The most efficient production of zeolites with high cation-exchange capacity (about 220 cmol/kg) is obtained after leaching the sludge ash in solutions of around pH = 3. At this low pH, gehlenite has already dissolved out of the sludge ash, half the Ca content of the ash has been leached out, Si has not yet been leached, but Al has begun to be leached. After ash zeolitization, LTA coexists with Na-P1 in the product.

INTRODUCTION

During the manufacture of recycled paper, paper sludge is discharged as an industrial waste. The amount of sludge increases annually. To reduce its volume, this sludge is incinerated, which produces paper sludge ash. At present, although paper sludge ash is used as an additive to cement and as a material for artificial aggregates (Singh and Garg 1999; Kikuchi 2001), a large amount of the ash is disposed of by dumping. It has become more difficult to secure a sufficient amount of land for the waste disposal. It is, therefore, essential to develop new techniques of ash utilization for further recycling.

The conversion of the ash into zeolite has been investigated recently (Henmi 1989; Ishimoto and Yasuda 1997; Mun and Ahn 2001). In the conversion, aluminosilicate, which is a main component of the ash, is transformed into zeolites by reaction with alkalies. Because of their unique pore structures and ion-exchange properties, zeolites (including those synthesized from paper sludge ash) are applied to such tasks as water purification and soil improvement (Ishimoto et al. 2000, 2003).

Due to calcite included in paper as fillers, however, recent ash contains a high percentage of calcium in the form of anorthite and gehlenite. It is reported that ash with a high percentage of Ca can be converted into zeolites, but that the product has a low cation-exchange capacity (Catalfamo et al. 1994). Moreover, it also has been reported that Ca compounds in the ash prevent the separation of the production slurry into solid and liquid during the filtration and sedimentation process (Murayama et al. 2000). The reduction of Ca content, therefore, is an important issue for the production of desirable zeolite materials.

To control the Ca content for zeolite synthesis at low temperature (80 °C), we propose a Ca reduction process through pre-treatment of the paper-sludge ash by acid leaching. Many researchers have reported on production of zeolites from coal fly ash by means of different hydrothermal activation methods, such as classic alkali activation (Querol et al. 2001), alkali fusion (Shigemoto et al. 1993), and two-stage synthesis (Hollman et al. 1999). Little information is available, however, on pre-treatment of the raw materials (ashes) by acid leaching. Additionally, more information is needed about zeolite synthesis at low temperature (<100 ºC), which is less expensive than the production of zeolites under hydrothermal conditions (>100 ºC). We have studied the leaching conditions of paper-sludge ash, the synthesis of zeolites from this ash at low temperature, and the cation-exchange capacity of the resultant product with the objectives of (1) demonstrating the relationship between starting materials for synthesis and the resulting zeolite phases, and (2) establishing the best ash-treatment conditions for production of

* E-mail: wajima@ioes.saga-u.ac.jp

0003-004X/04/1112–1694$05.00

high cation-exchange capacity for the zeolites. We report the underlying chemistry in leaching and zeolite synthesis.

EXPERIMENTAL METHOD

The experimental procedure is shown in Figure 1. The raw material, paper-sludge ash, was treated with an acid solution (HCl), and the slurry was separated into a solid and a solution phase, in which a large portion of Ca was partitioned into the solution. The low-Ca, solid-phase residue was then reacted in the alkali solution to synthesize zeolites under the fixed conditions shown in the figure.

Paper-sludge ash

Paper-sludge ash (PSA) was obtained from one of the paper companies in Japan. The composition of the ash, determined by energy dispersive X-ray spectrometry (EDS, E-MAX, energy EX-200, Horiba), is listed in Table 1. The ash mainly consists of SiO_2, Al_2O_3, and CaO, and some lower-concentration impurities, such as Na, K, Mg, Fe, and Ti. The pollutants in paper sludge ash, such as Cr, Cd, Hg, Pb, As, Cu, and Zn, are very minor, which makes them of minimal concern for water-purification application of the resultant zeolites. However, the high content of Ca is not favorable for the synthesis of zeolites with high cation-exchange capacity.

Ash leaching by HCl solution

The ash was leached using HCl solutions with initial concentrations of 1–5 *M*. Ten to fifty grams of ash were added to 100 mL of HCl solution (see solid/liquid ratio in Table 2). This mixture was stirred for 24 h with a magnetic stirrer. The solid was separated from the solution by centrifugation, then washed with pure water, which was purified through reverse osmosis membranes using a Millipore Mill-Q Labo system, and dried at 60 °C overnight in a drying oven. Solid samples were analyzed by X-ray diffraction (Rint-2200U/PC-LH, Rigaku), energy dispersive X-ray spectrometry, and FT-IR spectrometry (FTS-155, BIO-LAB Laboratories). The concentrations of the leached elements in the solution (Si, Al, and Ca) were determined by an inductively coupled plasma method (SPS4000, SEIKO). The pH of each leachant after the acid treatment was measured by a pH meter (PH/ION METER F-23, Horiba).

TABLE 1. Chemical composition of paper sludge ash, determined by energy-dispersive X-ray spectrometry

	Oxide (wt%)	Minor elements (mg / kg)
SiO_2	40.9	
Al_2O_3	22.9	
CaO	25.8	
Na_2O	0.2	
K_2O	0.2	
MgO	6.9	
Fe_2O_3	1.3	
TiO_2	1.8	
Cr		N.D. (< 0.5)
Cd		N.D. (< 0.1)
Hg		N.D. (< 0.01)
Pb		8.3
As		N.D. (< 1)
Cu		130
Zn		480

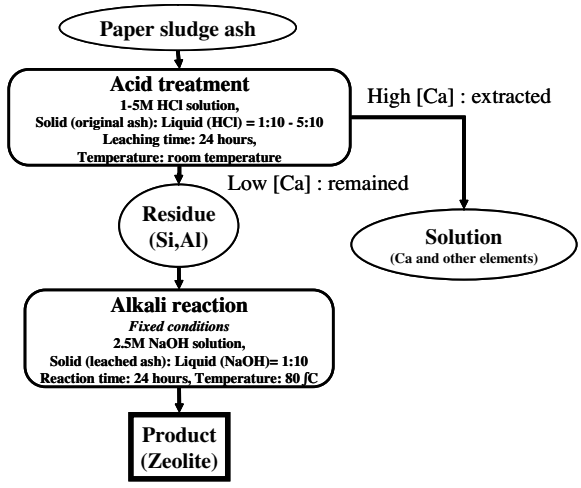

FIGURE 1. Flow chart of the experiments.

Zeolite synthesis from the leached ash

Raw paper-sludge ash and leached ashes, which were produced under each leaching condition mentioned above, then underwent the zeolitization process. Five g of each ash sample were added to 50 mL of 2.5 *M* NaOH solution in a 100 mL Erlenmeyer flask (made of polymethyl pentene) with a dimroth condenser. Zeolites formed from this alkali reaction under atmospheric pressure at 80 **°C** for 24 h. After the alkali reaction, the solid product was separated from the solution by filtration, then washed with pure water and dried at 60 **°C** overnight in a drying oven. The product was analyzed by XRD and scanning electron microscopy (S-2600H, Hitachi) to identify the zeolite phases.

Cation-exchange capacity of the product

The cation exchange capacity of the product was measured by the modified Schöerrenberg's method (DNUM 1994). The exchangeable cations in the product were replaced by NH_4^+ during immersion in 1 *M* ammonium acetate solutions, a procedure that was repeated three times. Then, the sample was washed with 80% EtOH in preparation for the next step of replacement. The NH_4^+ was replaced by K^+ in 10% KOH solution, in a procedure repeated three times. Finally, NH_4^+ in the solution was analyzed by the method of Koyama et al. (1976) to determine the cation-exchange capacity of the sample.

RESULTS

Conditions of leaching and properties of leached ash

The results of the leaching experiments are given in Tables 2 and 3. The first column in Table 2 shows the initial HCl concentration of the solution to which the ash is added; the second column (s/l) indicates the solid (ash)/liquid (HCl solution) ratio in which 10 to 50 g of raw ash were added to 100 mL of HCl solution, as mentioned above. The columns after the third show the chemical composition of leached ash, which was determined by EDS analysis. All leached ashes contain lower CaO and higher SiO_2 than the original ash. The results of acid leaching are listed in Table 3: the pH of the solution after 24 hours of acid leaching, the fraction of Ca extracted by leachant (ratio of the extracted Ca in the leachant to the original Ca content in the ash), and the residual mineral phases in leached ashes, which were determined by XRD.

The results listed in Table 3 are also illustrated in Figure 2; the abscissa is the initial HCl concentration (mol/L) to which the solution was adjusted, and the ordinate is the solid/liquid ratio. Shown on Figure 2 are the isopleths of (1) pH of leachant after 24 hours of leaching, (2) fraction of Ca extracted by leachant, and (3) residual mineral phases in the ash. With decreasing final pH of the leachant (from top-left to bottom-right in Fig. 2a), as indicated by the arrow direction, the fraction of Ca extracted increases (Fig. 2b) and the number of residual mineral phases decreases (Fig. 2c). These results indicate that the pH value in the final solution is the major indicator of the stage of acid leaching. In other words, the fraction of Ca extracted and the identity of the residual mineral phases are well described by the final pH of the leachant. So, hereafter we can discuss the results of leaching as a function of pH of the leachant after 24 hours of leaching.

Figure 3 shows typical XRD patterns of the leached ash, with

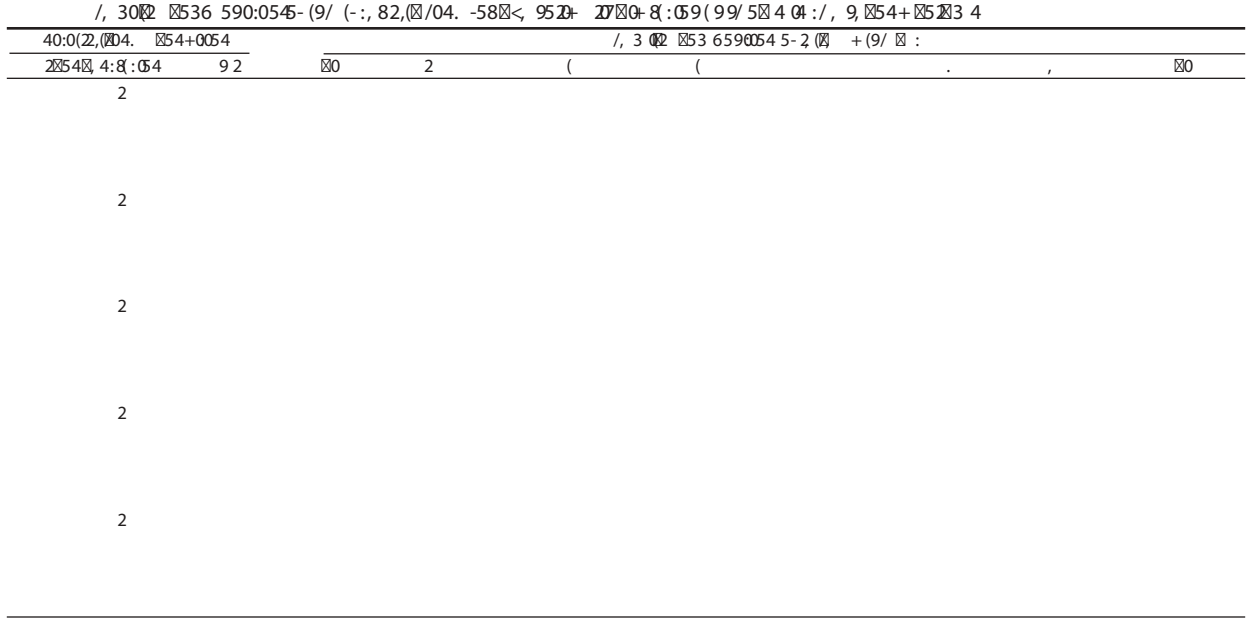

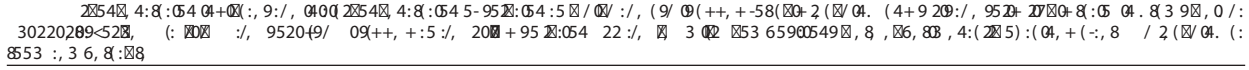

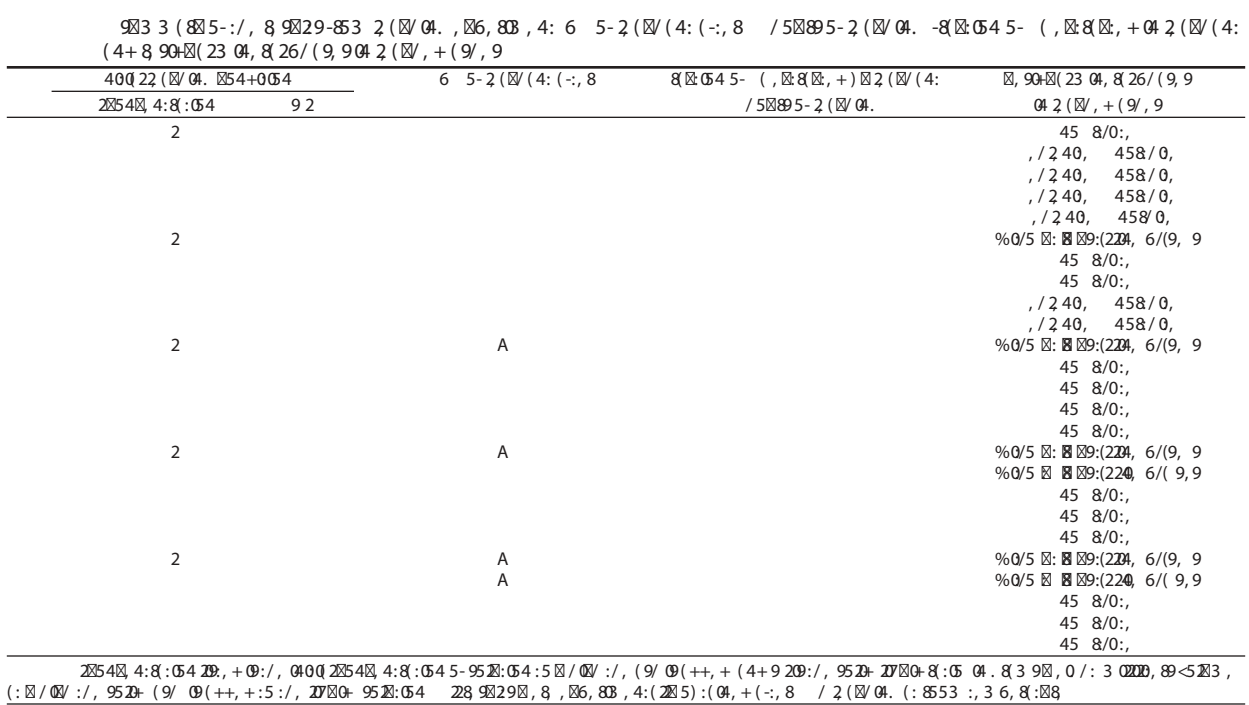

leachant pH indicated in the figure. It is observed that gehlenite and anorthite are the main crystalline substances in the starting ash. In the leachant at pH > 5, the concentration of gehlenite in the ash decreases with decreasing pH, and anorthite decreases from pH = 5 to pH = 1, as demonstrated by a weakening of their XRD peaks. Gehlenite dissolves out at pH = 5 and anorthite at pH = 1.

Figure 4 shows the individual fractions of Si, Al, and Ca extracted into the HCl solution compared to their original content in raw ash, vs. pH of the leachant. The concentrations of these leached elements were all measured experimentally, as mentioned above. It is clear that Si is hardly extracted at all over the whole pH range of the leachant. Aluminum starts to be extracted from about pH = 4 downward. Calcium is more efficiently extracted than the other two elements, and the fractional extraction increases in the lower pH regions. In the zeolite structure, the framework is composed of Si and Al, but Ca is not a main constituent of the structure. The most desired conditions are high [Ca] and low [Al] extractions, which cannot be met simultaneously. The figure suggests, however, that the

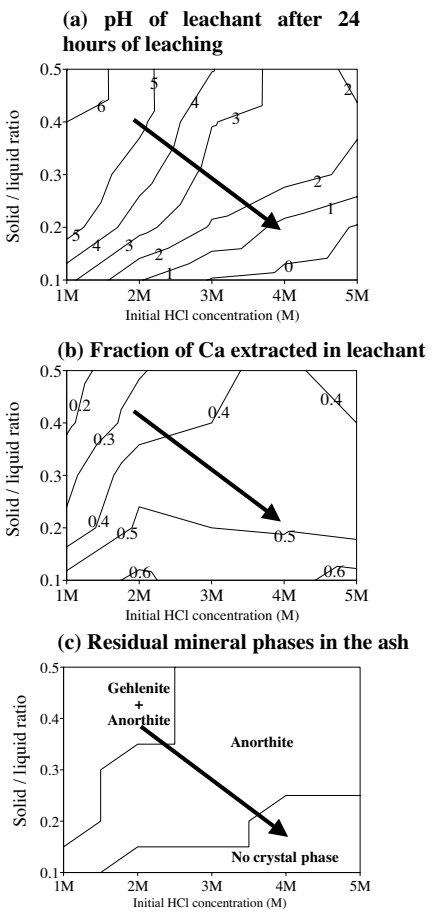

FIGURE 2. Identical trends (arrow direction in the figures) of **(a)** pH of leachant after 24 hours of leaching, **(b)** fraction of Ca extracted by leachant, and **(c)** residual mineral phases in the ash. All three figures are shown with the same abscissa and ordinate. The abscissa is initial HCl concentration of solution to which the ash is added for acid leaching, and the ordinate is the solid/liquid ratio (in g weight/ml volume), at which the solid (the ash) is initially added to the liquid (HCl solution).

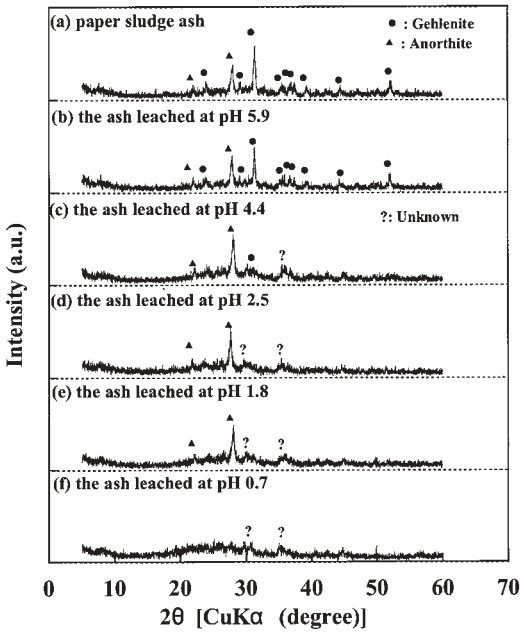

FIGURE 3. XRD patterns of raw paper-sludge ash and the leached ashes processed at the leachant pH indicated in the figure. Peaks of gehlenite are marked by solid circles, and those of anorthite by solid triangles. The peaks that are marked by "?" are of unidentified phases.

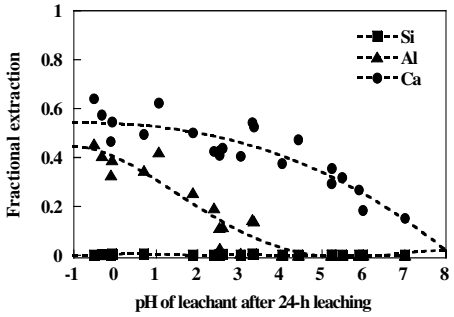

FIGURE 4. The fractional extractions of Si, Al, and Ca into leachant compared to their original content in raw ash, as a function of pH of leachant after 24-h leaching.

extractions should be done under conditions that produce a final leachant pH of around 3–4.

Figure 5 shows FT-IR spectra of original ash and the ash leached at a final pH of 3.3. The spectrum of leached ash shows four bands at 3380, 1640, 1100, and 920 cm^{-1}. Morrow et al. (1976) proposed that the reaction (Si-O-Si + $H_2O \rightarrow$ 2 Si-OH) occurred when a dehydroxylated silica was titrated with micromole doses of H_2O, and that a broad band centered near 3520 cm^{-1} accompanied the Si-OH formation. Lopez et al. (1992) reported IR spectra of a Ru/SiO_2 (0.5%) sample and they assigned the bands as follows: the 3580 cm^{-1} high-energy band is assigned to terminal silanols; an OH-bending band is observed at 1635 cm^{-1}; a typical Si-O stretching band and an Si-OH vibration are at 1078 and 985 cm^{-1}, respectively; and an Si-O-bending vibration appears at 805 cm^{-1}. Mendez-Vivar (1996) also reported IR spectra of silica xerogel doped with Mo (0.1 wt%). He assigned the bands as follows: the wide band centered on 3500 cm^{-1} corresponds to Si-OH bonds, with a shoulder appearing at 3200 cm^{-1} that corresponds to O-H bonds; the band at 1685 cm^{-1} is attributed to O-H bending; the intense signal at 1090 cm^{-1} is due to Si-O stretching bonds; and the band at 940 cm^{-1} is assigned to Si-OH of silanol groups that weakly bonded to the silica surface.

According to these reports, the present broad band centered at 3380 cm^{-1} corresponds to the band formed by the merging of two bands at 3500 and 3200 cm^{-1}, which are assigned to Si-OH and O-H bonds, respectively. The band at 1640 cm^{-1} is assigned to O-H bending. The intense band at 1100 cm^{-1} corresponds to Si-O stretching bonds with the shoulder at 920 cm^{-1} assigned to Si-OH silanols. As a whole, the bands appear to originate from silica gel. The four bands were observed in leached ash, but not in the original ash. The FT-IR spectra, therefore, clarify the formation of silica gel [$Si(OH)_4$] in the leaching process. This result explains why the Si remains in the solid in spite of the dissolution of two silicates, gehlenite and anorthite.

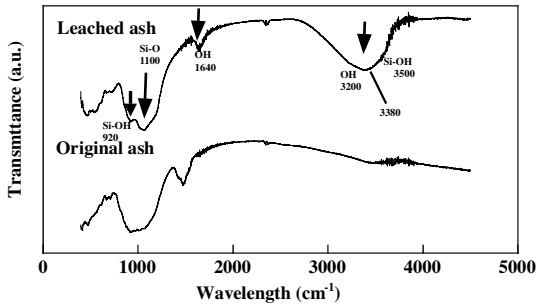

FIGURE 5. FT-IR spectra of original ash and the ash leached at a final pH of 3.3. Three arrows indicate 3300, 1640, and 1100 cm^{-1} bands, respectively, which appear to originate from silica gel.

Synthetic products and their cation exchange capacities

Figure 6 shows XRD patterns, as a function of final pH of the leachant, of the product synthesized from leached ashes through the alkali reaction at the fixed condition shown in Figure 1. Three types of zeolite—hydroxysodalite, LTA, and Na-P1—are observed, and are indicated by open circle, triangle, and square, respectively. The other phases, the peaks of which are marked by solid circle and triangle, are the residual minerals of leached ash, such as gehlenite and anorthite. As the pH of the leachant decreases, the product phase changes from hydroxysodalite to LTA, and finally to Na-P1. It is noted that a single phase of LTA is produced around pH = 4.5 and that of Na-P1 around pH = 2, as seen in Figures 6c and 6e, respectively, although these products also contain phases other than zeolite, such as residues or amorphous phases.

SEM photographs of (1) hydroxysodalite, (2) LTA, and (3) Na-P1 are shown in Figure 7. These figures demonstrate that each zeolite phase crystallizes in a different morphology. Linde Type A (LTA) ($Na_{12}Al_{12}Si_{12}O_{48}\cdot 27H_2O$, $Fm\bar{3}c$, a=24.6 Å) crystallizes in a typical cubic form. Its structural framework is built of 4- and 8-membered rings. Hydroxysodalite ($Na_6Al_6Si_6O_{24}\cdot 8H_2O$, cubic, $P\bar{4}3n$, a=8.9 Å) is a member of the sodalite group. Its structure comprises a framework of 4- and 6-membered rings of SiO_4 and AlO_4 tetrahedra. Na-P1 ($Na_6Si_{10}Al_6O_{32}\cdot 12H_2O$, cubic, $I\bar{4}$, a=10.0 Å) is a member of the gismondine group, and is also known as zeolite-P. Its structural framework is built of 4- and 8-membered rings. Note that both LTA and Na-P1 have 8-membered rings, larger than those in hydroxysodalite. The larger ring size correlates with greater cation-exchange capacity. Furthermore, the Si/Al ratio is higher in Na-P1 (Si:Al = 5:3) than in hydroxysodalite and LTA (Si:Al = 1:1). Because more Al is extracted at low pH, the high Si/Al ratio needed in the leached ash to form Na-P1 is consistent with its enhanced formation in the lower pH region.

The cation exchange capacity measured by the modified Schöerrenberg's method is shown in Figure 8 as a function of the pH of the leachant. The three symbols in the figure represent the residual mineral phases in the starting ash; the dotted lines, which are shown in the bottom of the figure, indicate the pH range of leached ash from which each zeolite phase was produced. Note that the data for three kinds of experiments, i.e., acid leaching, alkali reaction to produce zeolites, and cation exchange are illustrated together in the figure. The product with highest cation-exchange capacity is obtained around pH = 3, at which gehlenite has already dissolved out, anorthite has remained in the starting material, and LTA coexists with Na-P1 in the product.

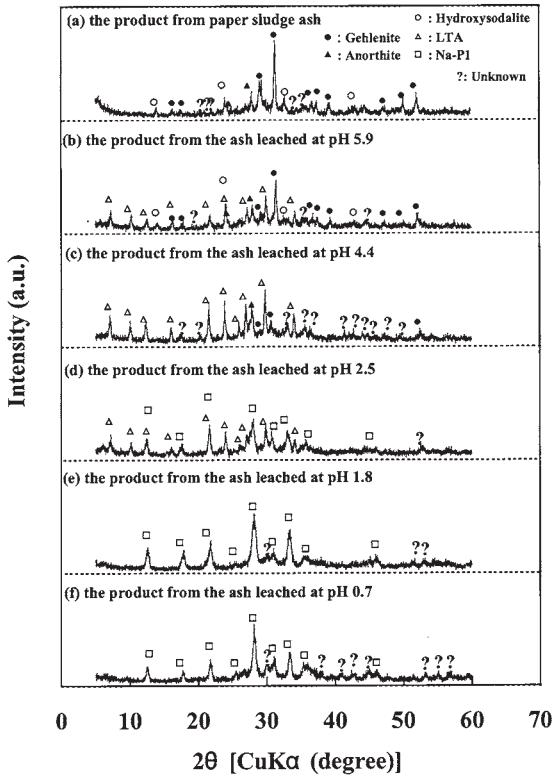

FIGURE 6. XRD patterns of the product synthesized after alkali reaction in 2.5 *M* NaOH solution for 24 h from raw paper-sludge ash and the ashes leached by the leachant at the final pH indicated in the figure. Peaks of hydroxysodalite, LTA, and Na-P1 are marked by open circle, triangle, and square, respectively. The peaks of the residual undissolved/unreacted minerals in the leached ash, such as gehlenite and anorthite, are marked by solid circle and triangle. The weak peaks that are marked by "?" sign are of unidentified phases.

DISCUSSION

Leaching mechanism and leaching condition

The chemistry of Ca, Si, and Al in the acid solution was well described by Kragten (1978). Calcium is present as Ca^{2+}, which is soluble, and Si is present as $Si(OH)_4$, which is insoluble. Accordingly, Ca can usually be leached, but Si is minimally leached by acid solution. Aluminum behaves in a manner different from Ca and Si. The extraction rate of Al dramatically increases below pH = 3–4. From pH = 7 to pH = 3–4, Al is stable in the form of $Al(OH)_3$, which precipitates from the solution, but below pH = 3–4, Al changes its speciation to form the Al^{3+} ion, which is soluble in the acid solution. Accordingly, in our study, Al dissolves in the solution at pH < 3–4.

The fractional extractions of Ca, Si, and Al in our study are in good accordance with the above general discussion as illustrated in Figure 4. In the present study, the formation of silica gel is also suggested by the IR-spectrum of leached ash shown in

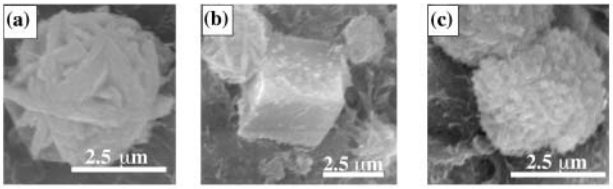

FIGURE 7. Scanning electron micrographs of zeolites, **(a)** hydroxysodalite synthesized from paper sludge ash, **(b)** LTA, and **(c)** Na-P1, synthesized from leached ashes.

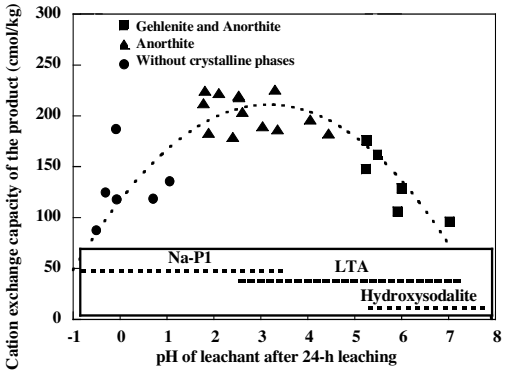

FIGURE 8. Cation-exchange capacities of the product synthesized from the ash leached by the leachant with final pH values as indicated in the abscissa. Three solid symbols, i.e., square, triangle, and circle, show the residual mineral assemblages in the leached ash. The dotted lines (in the bottom of figure) show the pH range of each zeolite phase in the product after the alkali reaction. Note that the zeolite ranges shown in the lower box only designate the presence of some amount of that zeolite; most of the products, however, are mixtures of zeolite(s) with additional substances.

Figure 5, which is consistent with the above discussion. But the mechanism of element extraction into solution is not so simple due to the differential solubility of minerals. Gehlenite is easier to dissolve than anorthite. It has completely dissolved out by about pH = 5, whereas anorthite only starts to dissolve. The form of Al changes from $Al(OH)_3$ to Al^{3+} at pH = 3–4. It is, therefore, reasonable that a pH just below 4 is a critical point for element extraction and mineral dissolution.

In summary, we propose the following mechanism for acid leaching, as shown in Figure 9. As leachant pH progresses downward, in the pH region just above 3-4, most gehlenite has already dissolved in the solution, but a large proportion of anorthite still remains in the solid phase. The main ions, Ca^{2+}, Al^{3+}, and Si^{4+}, of gehlenite are initially extracted into the solution, but Al^{3+} and Si^{4+} precipitate as $Al(OH)_3$ and $Si(OH)_4$ gels, leaving Ca^{2+} in the solution. In the pH region just below 3-4, all gehlenite and a large proportion of anorthite have dissolved into the solution; all three ions (Ca^{2+}, Al^{3+}, and Si^{4+}) are initially extracted by the solution, but Si^{4+} precipitates into a solid phase in the form of $Si(OH)_4$, leaving Ca^{2+}. A large proportion of Al precipitates in the solid, but some portion of Al remains in the solution.

It is, therefore, concluded that acid treatment around pH = 3 is appropriate to produce a solid residue with decreased Ca and high Al and Si for the purpose of generating zeolites.

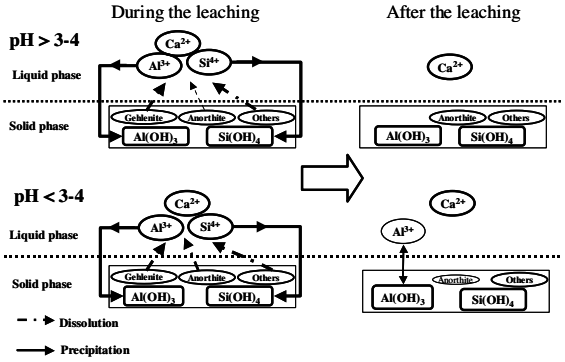

FIGURE 9. Proposed leaching mechanism of paper-sludge ash at pH > 3–4 (upper) and pH < 3–4 (lower). The dashed arrow indicates dissolution from the ash into the solution, and the solid arrow indicates precipitation from the solution to the ash. Note that, just above pH = 3–4, a large portion of anorthite does not dissolve. Moreover, all the Al that has dissolved, mainly from gehlenite, precipitated as solid $Al(OH)_3$, leaving only Ca^{2+} in the solution. In contrast, just below pH = 3–4, a large portion of anorthite dissolves, but most of the Al re-precipitates as a solid, leaving only a small portion of Al in the solution.

Leached ash and synthetic product

The cation-exchange capacity of the product is shown in Figure 8 as a function of the pH of the leachant, together with the residual mineral phases of leached ash and zeolite products. The leached ash contains both gehlenite and anorthite at pH > 5. At pH < 5, gehlenite dissolves out. The ash only contains anorthite without gehlenite for pH = 1–5. Anorthite content decreases with decreasing pH of leachant. For pH < 1, both of the minerals dissolve out, and the ash contains only non-crystalline phases. The products after the alkali reaction change from hydroxysodalite to LTA and to Na-P1 with decreasing pH of leachant. The maximum in the cation exchange capacity shows that the preferred zeolite product is synthesized from ash that is leached by a solution at pH = 3. The highest CEC of the product is about 220 cmol/kg, which is lower than that of commercial synthetic zeolite A or Na-P1 (about 400–500 cmol/kg), because the product is not synthesized from the ideal starting material for zeolites but rather from paper-sludge ash, and the product is composed of a mixture of synthetic zeolite phases and unknown, amorphous and unreacted substances.

The main components of paper sludge ash and leached ashes are Si, Al, and Ca. Figure 10 shows these main components of paper sludge ash and the leached ash in the ternary diagram having a single component at each corner. The leached ashes are divided into two regions. In Region I, the ash contains both residual gehlenite and anorthite, and the relative increase of Si content in the ash correlates with Ca decrease with decreasing pH of leachant. With decreasing pH of leachant, the ash contains less gehlenite. Along this same composition path, the product changes from hydroxysodalite to LTA, and finally to Na-P1. As the gehlenite content decreases in the ash, the product gains higher cation-exchange capacity. It has been reported that LTA and Na-P1 yield higher cation exchange capacity than hydroxy-

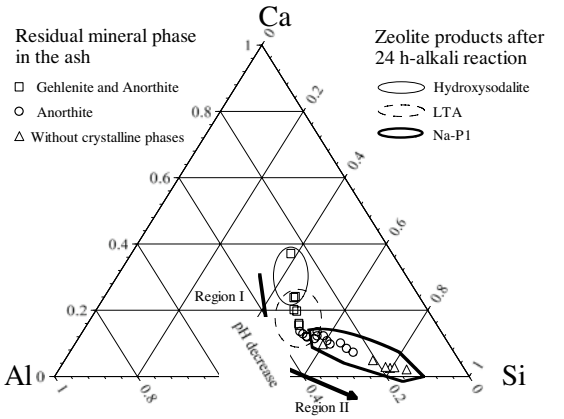

FIGURE 10. The Si-Al-Ca ternary diagram with the composition of original and leached ashes indicated. Three symbols, open square, circle, and triangle, indicate the residual mineral assemblages in the ash. Three zones enclosed by thin, dashed, and bold lines indicate the areas in which hydroxysodalite, LTA, and Na-P1 were synthesized by the alkali reaction, respectively. The arrows of Regions I and II indicate the direction in which the chemical composition shifted with decreasing pH of the final leachant.

sodalite (Hollman et al. 1999; Querol et al. 2002), which is consistent with the relative framework ring size. In Region II, the ash contains no gehlenite; with decreasing pH of leachant, the increase in Si content of the ash correlates with Al decrease. The ash contains less anorthite as the pH of the leachant decreases, and the product becomes Na-P1, which is consistent with the higher Si/Al ratio of the framework. The product develops lower cation-exchange capacity as the anorthite content decreases in the ash. The reason for cation exchange capacity decrease in Region II is that the production of Na-P1 decreases with the shortage of Al. Therefore, the best condition for high cation-exchange capacity is at the point that the leached ash contains only anorthite, in the boundary between Regions I and II.

ACKNOWLEDGMENTS

We thank two anonymous reviewers and the associate editor, Jill Pasteris, for improving our manuscript, and Robert Downs of University of Arizona and Shohei Banno, Emeritus Prof. of Kyoto University, for revising English in our manuscript.

REFERNCES CITED

Catalfamo, P., Patane, G., Primerano, P., Di Pasquale, S., and Corigliano, F. (1994) The presence of calcium in the hydrothermal conversion of amorphous alminosilicates into zeolite: Interference and removal. Materials Engineering, 5, 159–173.

Henmi, T. (1989) A physico-chemical study of industrial solid wastes as renewable resource—Zeolitization of coal clinker ash and paper sludge incineration ash. Memoirs of the faculty of Agriculture, Ehime University, 33, 143–149 (in Japanese with English abstract).

Hollman, G.G., Steenbruggen, G., and Janssen-Jurkovicova, M. (1999) A two-step process for the synthesis of zeolites from coal fly ash. Fuel, 78, 1225–1230.

Ishimoto, H. and Yasuda, M. (1997) Technology for converting papermaking sludge into micro-porous crystal materials. NTT REVIEW, 9, 51–56.

Ishimoto, H., Origuchi, T., and Yasuda, M. (2000) Use of papermaking sludge as new material. Journal of Materials in Civil Engineering, 12, 310–313.

Ishimoto, H., Yasuda, M., and Sasaki, O. (2003) Application of new materials from paper recycling for purifying domestic wastewater. NTT REVIEW, 15, 43–47.

Kikuchi, R. (2001) Recycling of municipal solid waste for cement production: Pilot-scale test for transforming incineration ash of solid waste into cement clinker. Resources, Conservation and Recycling, 31, 137–147.

Koyama, M., Hori, T., and Kitayama, Y. (1976) IARC Reports, Kyoto University, 2, 11–14.

Kragten, J. (1978) Atlas of Metal-ligand Equilibria in Aqueous Solution, Ellis Horwood Limited, Chichester.

López, T., Herrera, L., Mendez-Vivar, J., Bosch, R., Gómez, R., and Gonzalez, R.D. (1992) Support effect in ruthenium sol-gel catalysts on silica and alumina. Journal of Non-Crystalline Solids, 147–8, 773–777.

Mendez-Vivar, J. (1996) Spectroscopic study of molybdenum oxides supported on silica. Materials Chemistry and Physics, 43, 140–144.

Morrow, B.A., Cody, I.A., and Lee, L.S.M. (1976) Infrared studies of reactions on oxide surfaces. 7. Mechanism of the adsorption of water and ammonia on dehydroxylated silica. Journal of Physical Chemistry, 80, 2761–2767.

Mun, S.P. and Ahn, B.J. (2001) Chemical conversion of paper sludge incineration ash into synthetic zeolite. Journal of Industrial Engineering Chemistry, 7, 292–298.

Murayama, N., Ishimoto, H., and Shibata, J. (2000) Hydrothermal synthesis and physical property evaluation of zeolite from paper sludge ash. Journal of the Mining and Materials Processing Institute of Japan, 116, 31–36 (in Japanese with English abstract).

Development of New Utilization of Materials (DNUM) (1994) Natural Zeolite and its Utilization, p. 318–325. No. 111 committee, Japan Society for the Promotion of Science, Tokyo.

Querol, X., Umana, J.C., Plana, F., Alastuey, A., Lopez-Soler, A., Medinaceli, A., Valero, A., Domingo, M.J., and Gracia-Rojo, E. (2001) Synthesis of Na zeolites from fly ash in a pilot plant scale: Examples of potential environmental applications. Fuel, 80, 857–865.

Querol, X., Moreno, N., Umana, J.C., Alastuey, A., Hernandez, E., Lopez-Soler, A., and Plana, F. (2002) Synthesis of zeolites from coal fly ash: An overview. International Journal of Coal Geology, 50, 413–423.

Shigemoto, N., Hayashi, H., and Miyamura, K. (1993) Selective formation of Na-X zeolite from coal fly ash by fusion with sodium hydroxide prior to hydrothermal reaction. Journal of Materials Science, 28, 4781–4786.

Singh, M. and Garg, M. (1999) Cementitious binder from fly ash and other industrial wastes. Cement and Concrete Research, 29, 309–314.

MANUSCRIPT RECEIVED OCTOBER 17, 2003
MANUSCRIPT ACCEPTED JULY 26, 2004
MANUSCRIPT HANDLED BY JILL PASTERIS